Fish & Shellfish Immunology
January 2017, Volume 60, Pages 255-264
http://dx.doi.org/10.1016/j.fsi.2016.11.017
http://archimer.ifremer.fr/doc/00357/46800/

Immune priming and portal of entry effectors improve response to vibrio infection in a resistant population of the European abalone

Dubief Bruno [1, *], Nunes Flavia [1, 2], Basuyaux Olivier [3], Paillard Christine [1]

[1] Laboratoire des Sciences de l'Environment Marin (LEMAR), UMR6539, CNRS/UBO/IRD/Ifremer, Institut Universitaire Européen de la Mer, University of Brest (UBO), Université Européenne de Bretagne (UEB), Place Nicolas Copernic, 29280, Plouzané, France
[2] Ifremer Centre de Bretagne, DYNECO, Laboratoire d'Ecologie Benthique Côtière (LEBCO), 29280, Plouzané, France
[3] Synergie Mer et Littoral, Centre Expérimental ZAC de Blainville, 50560, Blainville-sur-mer, France

* Corresponding author : Bruno Dubief, email address : bruno.dubief@univ-brest.fr

Abstract :

Since 1997, populations of the European abalone *Haliotis tuberculata* suffer mass mortalities attributed to the bacterium *Vibrio harveyi*. These mortalities occur at the spawning season, when the abalone immune system is depressed, and when temperatures exceed 17 °C, leading to favorable conditions for *V. harveyi* proliferation. In order to identify mechanisms of disease resistance, experimental successive infections were carried out on two geographically distinct populations: one that has suffered recurrent mortalities (Saint-Malo) and one that has not been impacted by the disease (Molène). Furthermore, abalone surviving these two successive bacterial challenges and uninfected abalone were used for several post-infection analyses. The Saint-Malo population was found to be resistant to *V. harveyi* infection, with a survival rate of 95% compared to 51% for Molène. While *in vitro* quantification of phagocytosis by flow cytometry showed strong inhibition following the first infection, no inhibition of phagocytosis was observed following the second infection for Saint-Malo, suggesting an immune priming effect. Moreover, assays of phagocytosis of GFP-labelled *V. harveyi* performed two months post-infection show an inhibition of phagocytosis by extracellular products of *V. harveyi* for uninfected abalone, while no effect was observed for previously infected abalone from Saint-Malo, suggesting that the effects of immune priming may last upwards of two months. Detection of *V. harveyi* by qPCR showed that a significantly greater number of abalone from the susceptible population were positive for *V. harveyi* in the gills, indicating that portal of entry effectors may play a role in resistance to the disease. Collectively, these results suggest a potential synergistic effect of gills and haemolymph in the resistance of *H. tuberculata* against *V. harveyi* with an important involvement of the gills, the portal of entry of the bacteria.

Highlights

► Susceptibility to vibriosis differs between abalone from two distinct populations. ► Immune priming is observed in abalone following a first exposure to *V. harveyi*. ► The detection of *V. harveyi* is lower in the gills of resistant abalone. ► The growth rate of *V. harveyi* was lower in the serum of resistant abalone. ► Both portal of entry and haemolymph effectors may play a role in resistance.

Keywords : Immunity, Haemocyte, Abalone, Disease, Extracellular products, Immune priming, *Vibrio harveyi*, flow cytometry, Resistance, Phagocytosis, Bacterial growth, qPCR, Gill

1. Introduction

In the natural environment, the interaction between pathogens and their hosts has important evolutionary repercussions, influencing genetic diversity of both hosts and pathogens [1,2]. According to the Red Queen hypothesis, each partner of this couple is in constant antagonist coevolution where pathogens evolve new arms to colonize the host, who in turn develop new features to counteract them. In a stable environment, this arms-race can lead to a balance that prevents one taking advantage over the other. However, global change has the potential to disturb this power relationship. Rapid environmental change can favor pathogens that have shorter generation times than hosts, and thus may adapt to new conditions more quickly whereas the hosts are weakened by them. Among new stressors, global warming is an important factor implicated in the emergence of disease [3,4], with adverse consequences for biodiversity. Many pathogenic bacteria grow preferentially in warm seawater, which can lead to an increase in the prevalence of disease with increasing temperature [5,6]. Increasing temperatures can also be detrimental to the immune system of invertebrate hosts thereby facilitating infection by a pathogen. For example, temperature increase leads to a reduction in phagocytosis and phenoloxidase in *Haliotis diversicolor* infected with *Vibrio parahaemolyticus* [4]. Similarly, temperature increase leads to a reduction in phagocytosis and superoxide dismutase activity, while an increase in total haemocyte count is observed in the hard clam *Chamelea gallina* [7]. Rising global temperatures can therefore affect both pathogen and host, potentially generating more favorable conditions for disease.

The onset of massive mortalities of the European abalone *Haliotis tububerculata* is a compelling example of the de-stabilizing effects of environmental change on host-pathogen interactions. Since 1997, recurrent abalone mortality events of 50 to 90% have been attributed to the bacterium *V. harveyi* [8]. Field observations and laboratory studies of the disease etiology point to increasing water temperatures as the main cause of the disease. The first known mortalities were reported between Le Trieux and Saint-Malo, where

summer temperatures are among the highest in northern Brittany, France [9]. Subsequent disease outbreaks were limited to areas where summer temperatures exceeded 17.5°C [10]. In support of these field observations, experimental infections showed that *V. harveyi* was only able to cause death by septicemia when water temperatures exceeded 17°C during the spawning period of *H. tuberculata* [11]. In addition to temperature, gonadal maturation and spawning of *H. tuberculata* were found to be linked with immune depression characterized by a decrease in phagocytosis and phenoloxydase activity leading to greater susceptibility to the disease [12]. Other external stressors have also been found to lead to immune depression rendering *H. tuberculata* susceptible to disease [13]. However, while the combined effects of higher temperature and gametogenesis are required to trigger an infection in *H. tuberculata*, below 18°C, *V. harveyi* did not cause mortality in mature abalones [11], showing that temperature remains a key factor for the existence of the disease.

Given the rapid increase of sea surface temperatures [14] and the threat that it represents regarding the evolution of host-pathogen interactions, understanding whether and how marine organisms can defend themselves is of great concern. In the case of *H. tuberculata* infected with *V. harveyi*, the abalone immune system is rapidly affected by the pathogen, as already in the early stages of disease, phagocytosis, the haemocyte density and the production of reactive oxygen species are negatively impacted [15]. Moreover, *V. harveyi* can inhibit phagocytosis by inactivating p38 MAP kinase [16], avoiding the host immune system. While *V. harveyi* appears well-equipped to attack its host, less is known about the potential ability of *H. tuberculata* to defend itself against *V. harveyi*, and whether resistance to the disease exists. A successive infection experiment conducted on farmed abalone that aimed to select resistant individuals and identify potential effectors of resistance found that survivors over-expressed several genes implicated in metabolic regulation [17]. Because coping with stress such as gametogenesis and bacterial infection has an energetic cost, resistance to disease may therefore, be associated with individual or populational differences in metabolism and/or energy allocation strategies.

In the natural environment, recurrent mortality can select for disease resistance. In the black abalone *Haliotis cracherodii*, resistance against a rickettsial disease was found in the population of San Nicolas Island, which was historically the most impacted by the disease [18]. With respect to *H. tuberculata*, contrasting mortalities have been observed in natural populations in France, raising the question of whether resistant

86 populations can be found in areas highly impacted by the disease. Identification of a population tolerant or
87 resistant to the disease could allow resistance factors to be identified.

88 An additional feature of the invertebrate immune system that can lead to an improved response
89 against a pathogen is immune priming. Immune priming is an adaptive response of the immune system which
90 provides protection in a similar way to the immune memory of vertebrates, but via different biologic
91 mechanisms [19]. Invertebrate immune priming has been observed to be either a specific recognition of a
92 pathogen that then leads to a faster and more intensive immune response at a second exposure [19] or a
93 sustained non-specific immune response following a first infection [20]. In certain species, the enhanced
94 immunity stimulated by priming can be transmitted to the next generation, providing an important advantage
95 to the host in the context of emergent diseases [21]. Immune priming, if present in *H. tuberculata*, could be an
96 important defense against *V. harveyi*.

97 The main objectives of this study were (1) to examine the existence of a population of *H. tuberculata*
98 resistant to *V. harveyi* infection; (2) to compare the immune responses of different natural populations during
99 successive exposures to the pathogen, in order to explain differences in tolerance to the disease and (3) to
100 investigate a potential immune priming response of *H. tuberculata* against *V. harveyi*.

101

102 **2. Methods**

103 *2.1 Abalone and bacterial strains*

104 In order to identify populations with different susceptibilities to the disease, abalones were sampled in
105 an area that has been recurrently impacted by the disease (Saint-Malo) and in a non-impacted area (Molène).
106 Individuals from the two abalone populations were supplied by local commercial fishermen in May 2014: Saint-
107 Malo (weight 84.5 ± 14.3 g; shell length 83.1 ± 7.6 mm) and Molène (weight 82.5 ± 19.1 g; shell length 84.2 ±
108 4.4 mm). Abalones from the two populations were kept separate, but under the same controlled conditions for
109 approximately five months and fed with *Palmaria palmata* ad libitum. During this period, the two populations
110 received the same circulating water and the temperature was controlled such that the two populations reached
111 maturity at the same time and as close as possible to the first infection (1300 degree-days). Abalones were
112 transferred to infection tanks two weeks before the start of experimentation (September 2014). The
113 temperature was set to 17°C ten days before experimentation and then increased to 18°C four days before the

infection, in order to prevent uncontrolled bacterial proliferation prior to the experiment. Dead abalones were counted and removed twice daily.

The bacteria used for the challenge is a virulent strain of *Vibrio harveyi* (ORM4) isolated from diseased abalone in Normandy, France during an episode of massive mortalities in 1999 [8]. Bacteria were grown in Luria-Bertani Agar supplemented with salt (LBS) at a final concentration of 20g.l^{-1} during 72 hours at 18°C. Prior to use in the experiment, bacteria were washed with filter-sterilized seawater (FSSW) and quantified by optical density measurements at 490 nm. For the post-infection analyses, a modified mother strain of ORM4 was used: a kanamycin resistant strain, tagged with green fluorescent protein (GFP) [22].

2.2 Bacterial challenge

Abalones were challenged by two successive infections by immersion separated by a period of four weeks including three weeks of rest. They were placed in 100 L tanks in a closed system, supplied with seawater maintained at 18°C with a summer photoperiod (16h day/8h night) for a number of 22 abalones per tank. For each of the two populations, two conditions were performed in triplicate: a control condition with no bacterial exposure and another condition exposed to 10^4 CFU.ml^{-1} of *V. harveyi* during 24 h. After the 24 h exposure, water in all the tanks was renewed at 100%, with subsequent water renewals of 50% taking place each day for the remainder of the infection. A second infection was performed with the surviving abalones 28 days after the first exposure, following the same protocol. During the infection periods, abalones were not fed, but feeding with *P. palmata* resumed during the three-week rest period between the two infections. Dead abalones were counted and removed twice daily. The second infection was followed for one week. After this period, all surviving infected abalones and uninfected (control) abalones were kept for an additional two months at 18°C with a summer photoperiod and fed with *P. palmata* for post-infection analyses.

2.3 Sampling of abalone hemolymph and tissues

In order to compare the immune response of the two populations at different time intervals of the disease and between the first and the second infection, live abalone were sampled at 1, 3 and 5 days after the first infection and at 0 (just before exposure), 1 and 3 days after the second infection. Particular attention was given to not sample moribund abalones. For the second infection, sampling at 1 day was only possible for the Saint-Malo population because mortality in the Molène population was too high, and the number of animals

remaining was insufficient for 3 sampling points. For each sampling time point, three abalones were taken from each replicate tank. Approximately 5 mL of hemolymph was collected from each animal with a sterile syringe. 300 µl of hemolymph were used immediately for *in vitro* phagocytosis and total haemocyte count, 500 µl was frozen at -20°C for the detection of *V. harveyi* by qPCR. All animals were dissected to collect the gills which were frozen in liquid nitrogen immediately.

2.4 In vitro phagocytosis index, viability and Total Haemocytes Count (THC)

Freshly collected hemolymph was used immediately for quantifying phagocytosis, total haemocyte count (THC) and viability by flow cytometry. Three technical replicates were run for each biological replicate.

2.4.1 Viability index and THC

50 µl was diluted in 150 µl of AASH supplemented with 1% of Sybr Green fluorescent dye and 1% of propidium iodide fluorescent dye in a 96-well round-bottom plate. After 20 min incubation at room temperature, the plate was analyzed by flow cytometry. While Sybr Green binds to all nucleic acids present in the sample, and is measured by green fluorescence, propidium iodide can bind only to dead cells that have suffered loss in membrane integrity and is measured by red fluorescence. The THC value was obtained by the number of events showing a green fluorescence divided by the flow rate. The viability index was determined as the percentage of haemocytes which did not show red fluorescence.

2.4.2 Phagocytosis index using fluorescent beads

50 µl of hemolymph was diluted in 100 µl of FSSW and distributed in a 96-well round-bottom plate. Haemocytes were allowed to adhere for 15 min, followed by the addition of 50 µl of 2.00 µm fluorescent beads diluted 1:100 in distilled water (Fluoresbrite YG Microspheres, Polysciences) [12]. After 1 h incubation at 18°C, the supernatant was removed and 50 µl of trypsin (2.5 mg.ml-1) in an anti-aggregating solution (AASH: 1.5% EDTA, 6.25 g L NaCl, in 0.1 M phosphate buffer, pH 7.4) was added to detach the cells from the bottom of the wells. After 10 min of shaking at the maximum speed on a Titramax 100 plate shaker (Heidolph), 150 µl of AASH was added and the plate was analyzed by flow cytometry with the Guava EasyCyte Plus (Merck Millepore). Beads were identified by their green fluorescence and the phagocytosis index was defined as the percentage of haemocytes phagocyting three or more beads.

172

173 *2.4.3 Detection of V. harveyi in hemolymph and gills by real-time quantitative PCR*

174 DNA was extracted from 500 µl total hemolymph, and from 30 mg of gill tissue using the QIAamp DNA
175 mini kit (QIAgen) according to the manufacturer's protocol. Hemolymph samples were centrifuged at 10 000g
176 for 10 min. Pellets containing bacteria and haemocytes were digested during 2 h with ATL buffer supplemented
177 with 20 µl proteinase K. Frozen gills were ground with a MM400 mixer mill (RETSCH) and kept frozen using
178 liquid nitrogen. After all subsequent steps of the standard protocol, the columns were eluted twice, first with
179 150 µl of DNase free water, then with 50 µl. In order to quantify *V. harveyi* in hemolymph, a standard curve was
180 obtained with 10-fold serial dilution in FSSW of *V. harveyi* bacterial culture, ranging from 10^8 to 0 CFU. In order
181 to obtain a standard curve for gill tissue, bacterial culture was mixed with uninfected gill tissue homogenate in
182 order to extract DNA under the same conditions as infected gill tissue. A 10-fold serial dilution of bacterial
183 culture from 10^7 to 0 CFU were added to an uninfected abalone gill homogenate of 30 $mg.ml^{-1}$. Bacteria
184 concentration was estimated using a Malassez counting chamber under light microscopy.

185 The concentration of *V. harveyi* was quantified by qPCR using the LightCycler 480 Probes Master
186 chemistry on a LightCycler 480 thermocycler (Roche). Amplification of the *V. harveyi tox-R* gene was done with
187 the following specific primers: ToxR F1 CCA-CTG-CTG-AGA-CAA-AAG-CA and ToxR R1 GTG-ATT-CTG-CAG-GGT-
188 TGG-TT. Fluorescent visualization of amplification was done using a *tox-R* probe dually labeled with the Texas
189 Red 5' reporter dye and the BHQ-2 downstream 3' quencher dye: CAG-CCG-TCG-AAC-AAG-CAC-CG [23]. Each
190 PCR reaction was run in triplicate, containing 5 µl of DNA, 600 nM of each primer, 200 nM of probes and 7.5 µl
191 of master mix, for a final volume of 15 µl. Thermal cycling consisted of an initial pre-incubation step at 95°C for
192 10 min, followed by 45 cycles of denaturation at 95°C for 10 s, annealing and extension at 58°C for 1 min and 30
193 s, the fluorescence reading at each cycle at 72°C for 1 second. The thresholds were set using LightCycler 480
194 software V 1.5 (Roche). The primer efficiency was determined by the slope of the standard curves using the
195 equation $E = 10^{(-1/slope)}$.

196

197 *2.5 Post-infection analyses*

198 Abalones surviving the experimental infections (from the Saint-Malo population) and uninfected
199 (control) abalones (from both Saint-Malo and Molène) were used for several additional analyses. No survivors
200 remained for the Molène population after two successive bacterial challenges. Additional analyses included: (1)

3D microscopy of intracellular uptake of *V. harveyi* by abalone haemocytes, (2) impact of extracellular products of *V. harveyi* on phagocytosis, and (3) the impact of abalone serum on bacterial growth. To minimize stress each individual was sampled for hemolymph only once.

2.5.1 3D Microscopy of phagocytosis

Because the methods in flow cytometry used here cannot distinguish whether bacteria are adhered to the surface of a haemocyte or are internalized into the haemocyte, intracellular uptake of *V. harveyi* by abalone haemocytes was confirmed by 3-dimensional fluorescence microscopy for abalone from both Saint-Malo and Molène. Freshly collected hemolymph was diluted ten times in FSSW (100µl) and allowed to adhere for 15 min on a glass slide. The supernatant was removed and replaced by a GFP *V. harveyi* suspension [22] to obtain a 50:1 bacteria to haemocyte ratio. After 1h of incubation at 18°C, the supernatant was removed and glass slides were washed twice with Phosphate Buffered Saline (PBS) pH 7.4 before being fixed for 10 min with 3.7% formalin in PBS. After two washing steps with PBS, glass slides were covered by 100 µl of a dilution of methanolic stock solution of rhodamine-phalloidin R415 (Invitrogen) with PBS for 20 min, in order to label the actin of cytoskeleton, washed again in PBS, and covered with 100 µl of 4′, 6-diamidino-2′-phenylindole, dihydrochloride (DAPI) at 0.1 $\mu g.ml^{-1}$ (Thermo Scientific) for 5 min, to label the nucleus. Finally, the slides were washed with PBS before observation. Slides were observed on an Axio Observer Z1 complemented by the 3D Vivatome module (Carl Zeiss AG). Lasers were used at λ_{ex} 494nm ± 20 for GFP (λ_{em} 436 ± 40), λ_{ex} 406 nm ±15 for DAPI (λ_{em} 457 ± 50), and λ_{ex} 575 nm ± 25 for rhodamine-phalloidin (λ_{em} 628 ± 40). In order to obtain a 3-dimensional image, series of 14 optical cross-sections of 0.8µm were collected and compiled. The images were processed with the AxioVision V 4.8 software (Carl Zeiss AG).

2.5.2 Impact of extracellular products of V. harveyi *on phagocytosis of GFP-labelled bacteria*

Bacterial extracellular products (ECPs) were produced by the cellophane overlay method [24]. Luria Bertani agar plates were covered with sterile cellophane films, and then 2 ml of approximately 10^9 *V. harveyi* culture was transferred to the top of the cellophane and incubated at 18°C for 72h. The bacteria and their ECPs were recovered by successive rinsing with 4 ml of FSSW. The ECP/bacteria suspension was centrifuged at 10000 g for 30 min, and the supernatant containing ECPs was recovered and filtered at 0.2 µm. ECP concentration was measured by the Bradford method [25], with serum albumin as the standard. Phagocytosis of GFP-labelled

V. harveyi was measured in the presence of two concentrations of ECPs: 15 and 30 µg.ml^{-1}, and a positive control of FSSW containing no ECPs (0 µg.ml^{-1}). Flow cytometry was performed on the Guava EasyCyte Plus (Merck Millepore). Phagocytosis values were represented by the mean of green fluorescence following the protocol described in Pichon et al. (2013), using 1 hour incubation.

2.5.3 Impact of abalone serum on bacteria growth

The ability of *V. harveyi* to grow in the serum of abalone from Molène and from Saint-Malo was tested using two strains: the virulent ORM4 and the non-virulent strain LMG 7890 [16]. For each abalone population, 1 ml of hemolymph from 5 individuals was pooled, and then centrifuged at 200 g for 10 min in order to recover only the serum, followed by filter-sterilization at 0.2 µm. Measurements of both ORM4 and LMG 7890 growth were done in 100-well flat-bottom plates with a computer-controlled incubator/reader/shaker, the Bioscreen C MBR. 150 µl of serum and 50 µl of bacteria suspension in LBS ($4{\cdot}10^4$ cells.ml^{-1}) were pipetted into each well. In order to have a stable control against which to compare bacterial growth in the serum of abalone from Molène and Saint-Malo, a positive control of growth was performed for both strains by adding 50 µl of bacteria suspension with 150 µl of LBS. A negative control was performed by adding 50 µl of sterile LBS with 150 µl of serum. Each condition was performed in triplicate. The plate was incubated at 18°C for 42 hours and the absorbance at 492 nm was measured at intervals of 30 min. The bacterial concentration was calculated with the following formula: $6 \cdot 10^9 \times OD + 2 \cdot 10^8$ [22]. The maximum growth rate for each condition was obtained by calculating the slope of the bacterial exponential growth phase from a plot of the natural logarithm of bacterial abundance versus incubation time.

2.6 Statistical analysis

The survival rate of infected and uninfected abalone from Saint-Malo and Molène was computed with a Kaplan-Meier estimate followed by a log-rank test in the R "survival" package[27]. Phagocytosis and THC data were fitted on a linear mixed effects model with the factor tanks as random effect, followed by a pairwise comparison of the least-squares means between uninfected and infected treatments. The effects of ECP on phagocytosis for each population were estimated by a 2-way nested ANOVA. As the hemolymph of each individual was used to quantify phagocytosis under three concentrations of ECPs (conditions 0, 15 and 30 µg.ml^{-1}), individuals were considered as repeated factors. Then pairwise comparisons of the least-squares

means between ECP treatments were performed. Finally, a logistic regression model was used to investigate the link between the phagocytosis index and the probability of abalone to be positive for *V. harveyi*; and to evaluate if there were differences in the probability of being positive for *V. harveyi* for abalone originating from Saint-Malo or Molène. In all tests, at the significance threshold was set to $\alpha = P < 0.05$. All statistical analyses were performed using the software R (version 3.2.3)[28].

3. Results

3.1 Differential survival of abalone following V. harveyi infection in Saint-Malo and Molène

The survival of abalones was measured in order to observe differences in resistance to infection with *V. harveyi* between the two populations. Indeed, during the first infection, the population of Molène suffered great mortalities whereas the population of Saint-Malo exhibited very little mortality. After the last observed mortality (24 days after the first exposure), the survival rate was 0.512 for Molène and 0.953 for Saint-Malo (Fig. 1). Survival for the Saint-Malo population was not significantly different from the uninfected controls (P=0.765). The log-rank test showed a significant difference in survival between the two infected populations (P<0.001). Survival was quantified only until 7 days after the second exposure, and by this time point no additional mortality was observed.

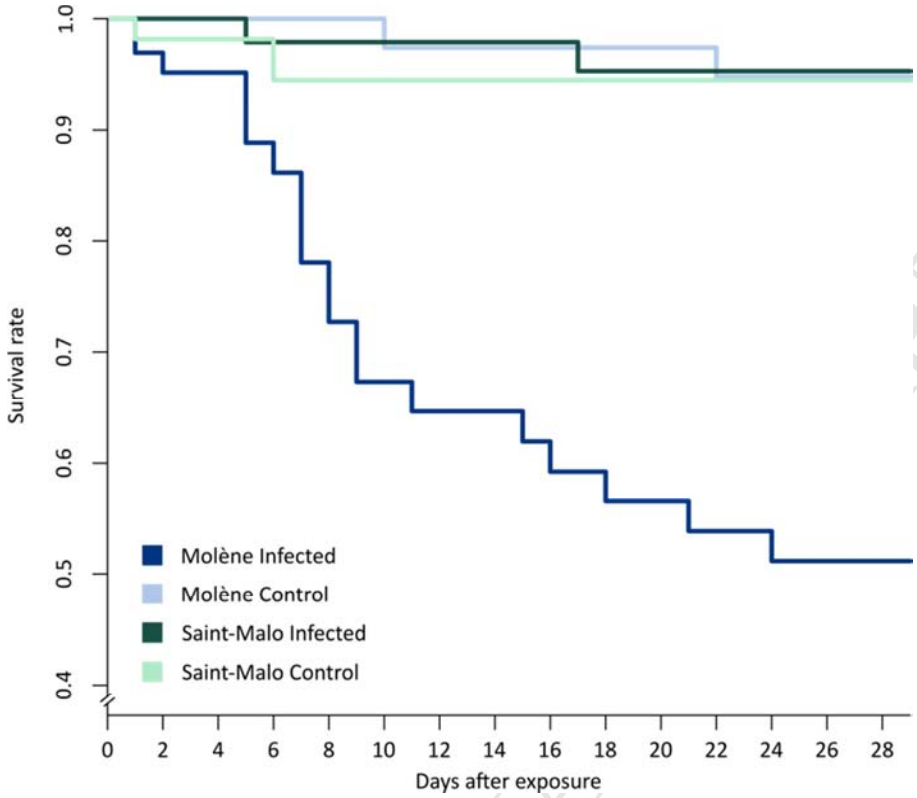

276

Fig. 1 : Kaplan-Meier survival rate following the first exposure of the two populations to 10^4 bacteria/mL during 24 hours at 18°C

277

278 *3.2 THC and Viability during the successive infections*

279 Total haemocyte count (THC) and haemocyte viability were measured for individuals from Saint-Malo
280 and Molène. Whereas no significant differences in THC were observed in abalones from Saint-Malo across all
281 time points, abalones from Molène exhibited a significant increase in THC after 24h of exposure (Fig. 2). A slight
282 decrease of THC was observed during the second infection for abalones from Saint-Malo but was not significant
283 (P=0.0947). No change was detected in the viability of haemocytes during the successive infections in both
284 populations. The mean of haemocyte viability was 98.44±0.09% across all individuals measured.

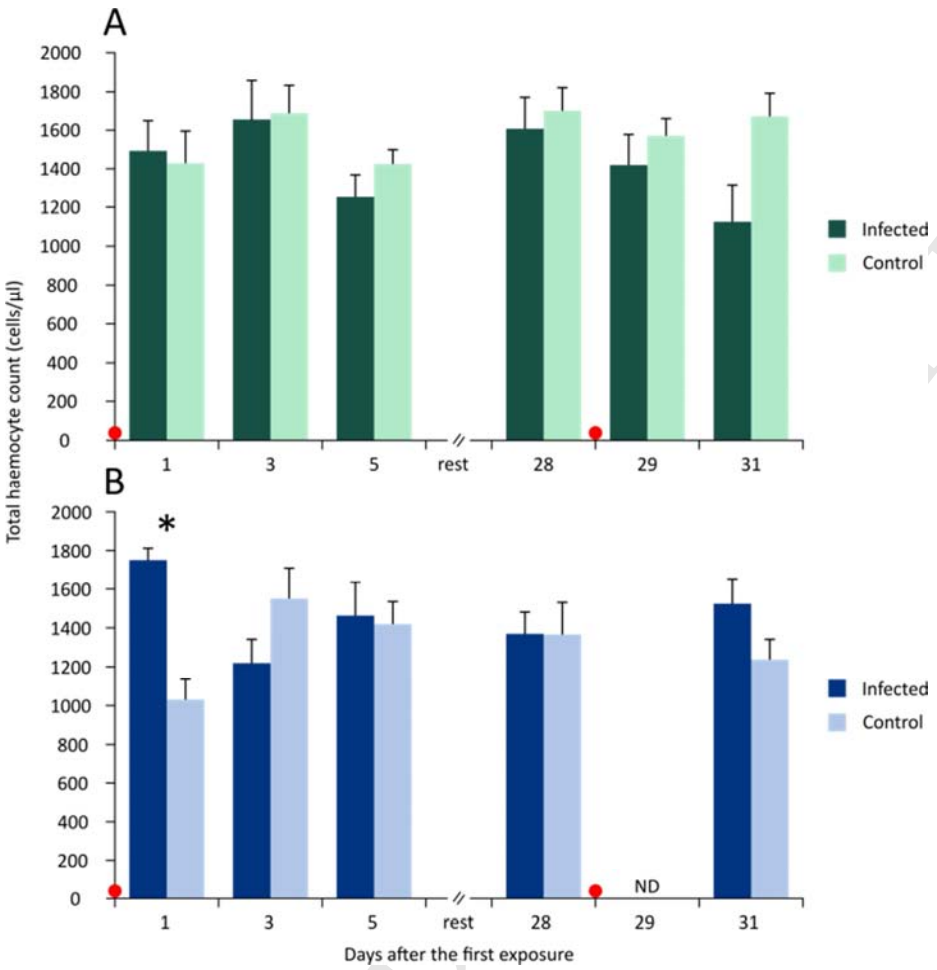

Fig. 2: Total haemocytes count (THC) during the two exposures of (A) Saint-Malo and (B) Molène. Red dots indicate the exposures. ND indicates that no data is available.* indicates values that are significantly different from the control for a pairwise comparison of the least-squares means ($p < 0.05$).

3.3 Phagocytosis index during the successive infections

A significant decrease in the phagocytosis index was observed 1 day after the first exposure to *V. harveyi*, of 36% for Molène and 40% for Saint-Malo, relative to the uninfected abalone (Fig. 3). By 2 days, the phagocytosis index of infected abalones recovered to the level of the uninfected controls and remained at the level of the controls until 5 days post-infection. Just prior to the second exposure, no significant difference in the phagocytosis index was observed between infected abalone and uninfected controls for the two populations. During the second infection, no reduction in phagocytosis was observed in the infected abalones from Saint-Malo and the level of phagocytosis was not significantly different than that of uninfected controls until the end of the experiment. In contrast, abalone from Molène showed a significant decrease in phagocytosis 5 days after the second exposure. (Fig. 3)

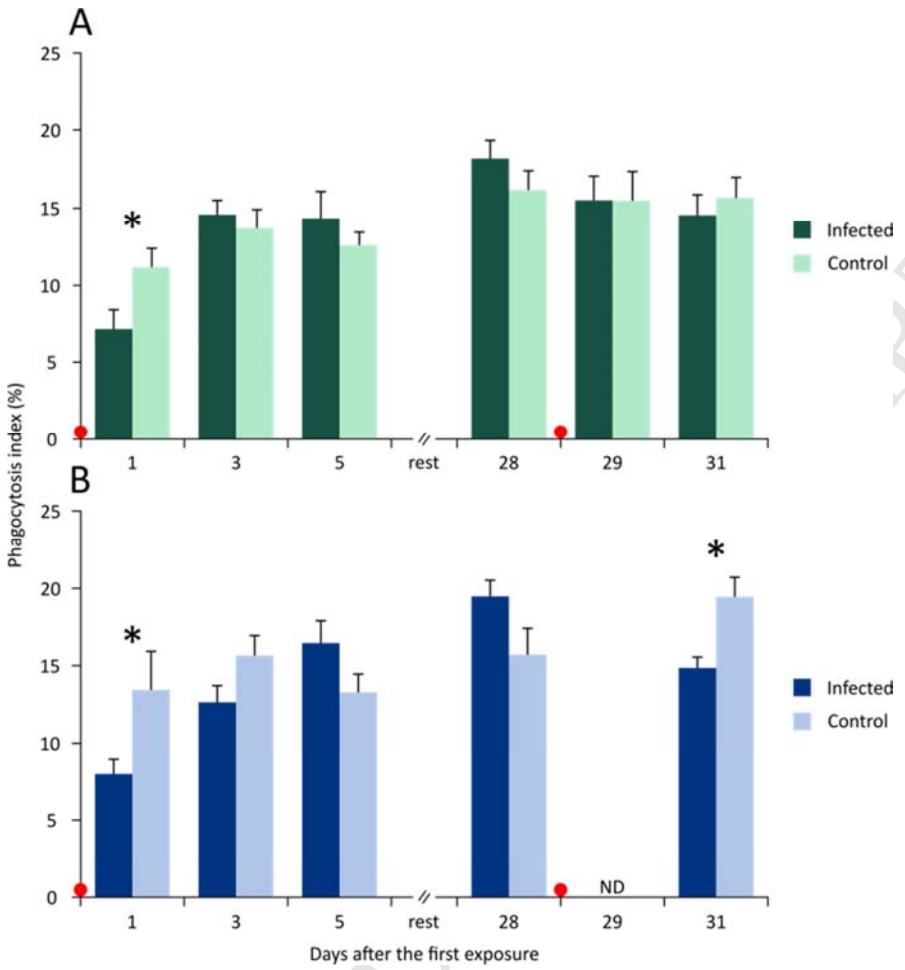

Fig. 3: Phagocytosis index based on micro-beads engulfment (percentage of haemocytes containing three or more fluorescent beads relative to total haemocytes) during two successive infections of abalone from (A) Saint-Malo and (B) Molène. Red dots indicate the timing of bacterial exposure. ND indicates that no data is available.* indicates values that are significantly different from the control for a pairwise comparison of the least-squares means ($p < 0.05$).

3.4 Detection of V. harveyi in hemolymph and gills by qPCR

The sensitivity threshold of qPCR was estimated to be $7.5 \cdot 10^2$ bacteria/ml of hemolymph and $2.5 \cdot 10^2$ bacteria/30 mg of tissue for gills. *V. harveyi* was detected in the gills of 20 individuals and in the hemolymph of 7 individuals (fig. 4). The concentration of bacteria was in the range of $5.51 \cdot 10^2 \pm 57$ bacteria/30 mg of gills and $6.4 \cdot 10^3 \pm 2.02 \cdot 10^3$ bacteria/ml of hemolymph. One individual showed $1.8 \cdot 10^4$ bacteria/ml of hemolymph, which explains the high standard deviation for this compartment (the average without this outlier individual was $4.52 \cdot 10^3 \pm 7.23 \cdot 10^2$ bacteria/ml of hemolymph). As the concentration of *V. harveyi* was near the detection threshold for most samples from which *V. harveyi* was detected, the detection results were treated as positive or negative for the presence of the bacterium. A binomial logistic regression was used to treat these results.

In the hemolymph, very few individuals were detected as positive for *V. harveyi*: 4 infected abalones from Molène and only 1 from Saint-Malo across all time points combined. Two uninfected control individuals (one in each population) were also detected as positive. *V. harveyi* was detected in the gills of a greater number of individuals: 15 positives in Molène and 5 in Saint-Malo with *V. harveyi* being detected in 1 uninfected control in the Molène population. The time points which exhibited the greatest number of positives were 1 day and 5 days after the first exposure. For all time points, the proportion of positive individuals was greater for Molène than for Saint-Malo. A logistic regression was consequently performed only on the infected abalones by taking into account 3 explanatory factors relating to the probability of abalones to be positive for *V. harveyi* on the gills: the phagocytosis index, the THC and the populations. All three factors significantly influenced the odds of abalone being positive for *V. harveyi*, with the odds of an abalone being positive for *V. harveyi* being 12.9 times higher in abalones from Molène.

Table 1: Logistic regression examining the effect of the population(pop), the phagocytosis index (phago) and the total haemocytes count (THC), on the proportion of abalones positive to V. harveyi on the gills. (*) For THC, the estimate and odds ratio are calculated for an increase of 500 cells/µL.

Coefficients:

	Estimate	odds ratio	std. Error	z value	Pr(>|z|)	
(Intercept)	-5,02786	0,00655282	2.19997	-2.285	0.02229	*
pop	2,55707	12,8979708	0.80107	3.192	0.00141	**
phago	-0,17121	0,8426446	0.07558	-2.265	0.02350	*
THC (*)	1,30651	3,69326171	0.50927	2.565	0.01030	*

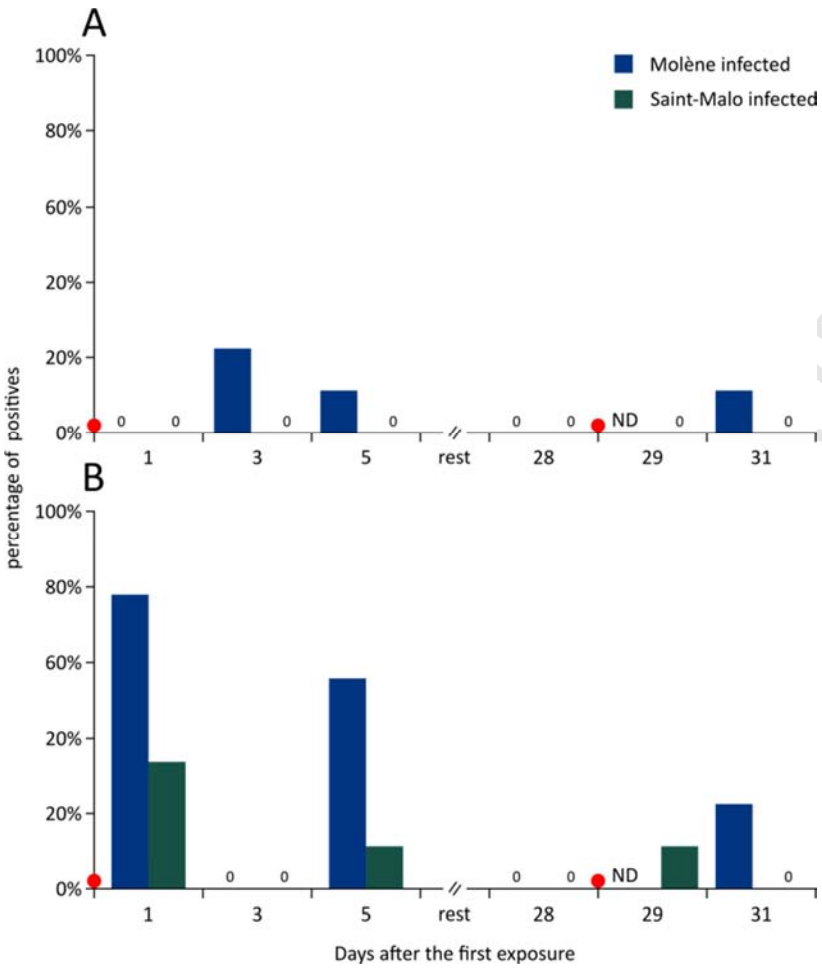

Fig. 4: Percentage of positive individuals for *V.harveyi* (n=9) in (A) haemolymph and (B) gills obtained by qPCR using specific primers and a TaqMan probe. The number 0 indicates that no individuals were found as positive at a given population and time point. Red dots indicate the timing of bacterial exposure. ND indicates that no data is available.

3.5 Post-infection analyses:

3.5.1 Fluorescence microscopy of phagocytosis

In order to validate that *V. harveyi* is internalized rather than adhered externally to abalone haemocytes, 3-dimensional fluorescence microscopy was carried out using individuals from Saint-Malo and Molène. Three-dimensional fluorescence microscopy shows that *V. harveyi* is well phagocyted by the haemocytes of *H. tuberculata* from the two populations. In Fig 5, the nucleus of the haemocyte is shown in blue and its cytoskeleton, delimiting the plasma membrane of haemocytes, is shown in orange. The green points observed to the left of the nucleus and within the cell membranes correspond to GFP-labelled *V. harveyi* located inside the cell. The flanking panels (Fig. 5 A, C), showing cross-sections of the haemocyte along the z-

and x-axes, confirm that bacteria are inside haemocyte cells and not merely at the surface. Similar images were obtained using haemocytes from individuals from both Saint-Malo and Molène.

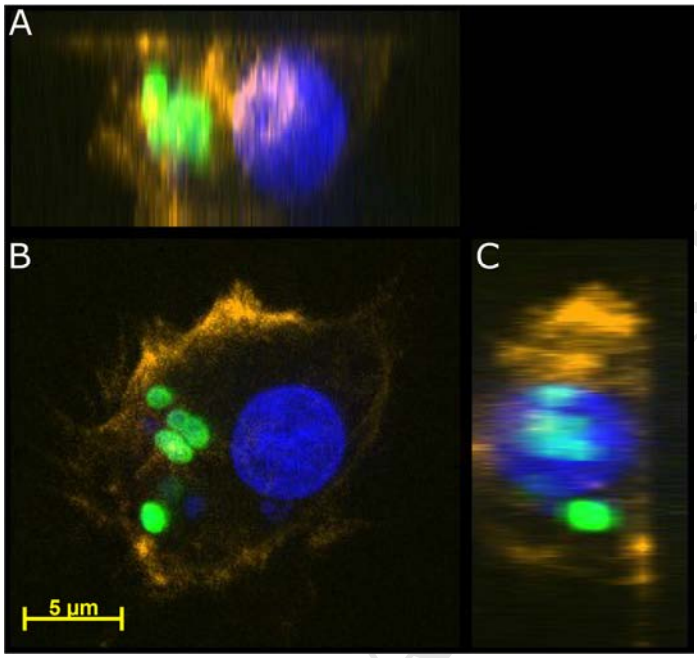

Fig. 5: 3-dimensional fluorescence microscopy (x60) pictures of a haemocyte (cytoskeleton in orange and nucleus in blue) which has phagocyted GFP-labelled *V. harveyi* (green). The central picture (B) shows a reconstruction of 14 stacked fluorescence images. The flanking pictures show cross-sections compiled along the (A) z-axis and (C) x-axis.

3.5.2 Effect of the V. harveyi ECPs on the capacities of abalone to phagocyte this bacteria

Haemocytes of abalones from each population were exposed to 0, 15 and 30 µg.ml^{-1} of ECPs obtained from the ORM4 strain of *V. harveyi*. Phagocytosis of GFP-labelled *V. harveyi* under exposure to ECPs was quantified two months after the successive infections experiment (Fig. 6). A nested ANOVA showed no significant differences between the Saint-Malo and Molène populations, but the factor ECPs exhibited a significant p-value < 0.001. Thus, pairwise comparisons of ls-means were performed within each population in order to evaluate their responses to ECPs treatments. A concentration of 30µg.ml^{-1} ECPs showed a significant negative effect on the phagocytosis index of uninfected individuals, with an inhibition of phagocytosis of 19% for abalone from Molène and 22.8% for Saint-Malo. Abalones from Saint-Malo having survived the successive infections showed no significant difference in phagocytosis when exposed to 0, 15 and 30 µg.ml^{-1} of ECPs.

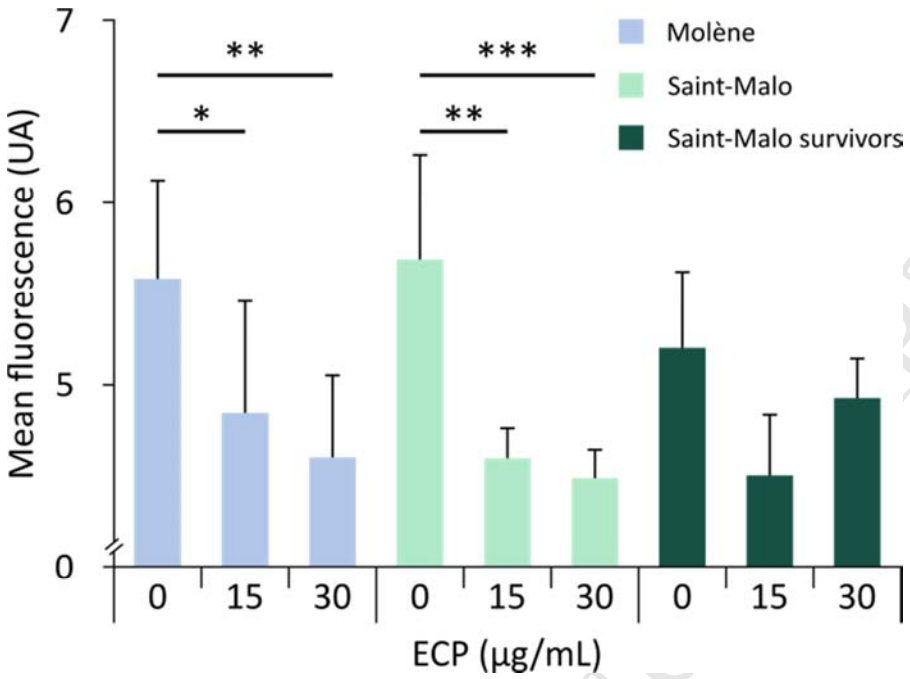

347

Fig. 6: Impact of two concentrations of extracellular products of *V. harveyi* (15µg/mL and 30 µg/mL) on phagocytosis of GFP-labelled bacteria. Values are the means of green fluorescence emitted by haemocytes. * indicates values that are significantly different from condition without ECPs for a pairwise comparison of the least-squares means (*P < 0.05, **P < 0.01, ***P < 0.001).

348

349 *3.5.3 Ability of V. harveyi to grow in acellular fraction of abalones hemolymph*

350 The growth of two strains of *V. harveyi* (LMG7890 and ORM4) in the acellular fraction of the
351 hemolymph from abalone of Saint-Malo and Molène were followed during 42 hours (Fig. 7). In order to have
352 the necessary volume of serum, hemolymph of five individuals was pooled for each population. The two
353 bacterial strains tested began their growth at approximately 2-3 hours earlier than in LBS, the positive control.
354 Growth rate was faster in the pathogenic strain (ORM4) relative to the non-pathogenic (LMG7890). Moreover,
355 the ability of *V. harveyi* to grow in abalone serum was lower in Saint-Malo (86% of the maximum growth rate
356 observed in LBS for uninfected abalone and 92% for survivors), while the growth rate in the serum of abalone
357 from Molène was nearly the same as in the LBS positive control (101% of the rate observed in LBS).

358

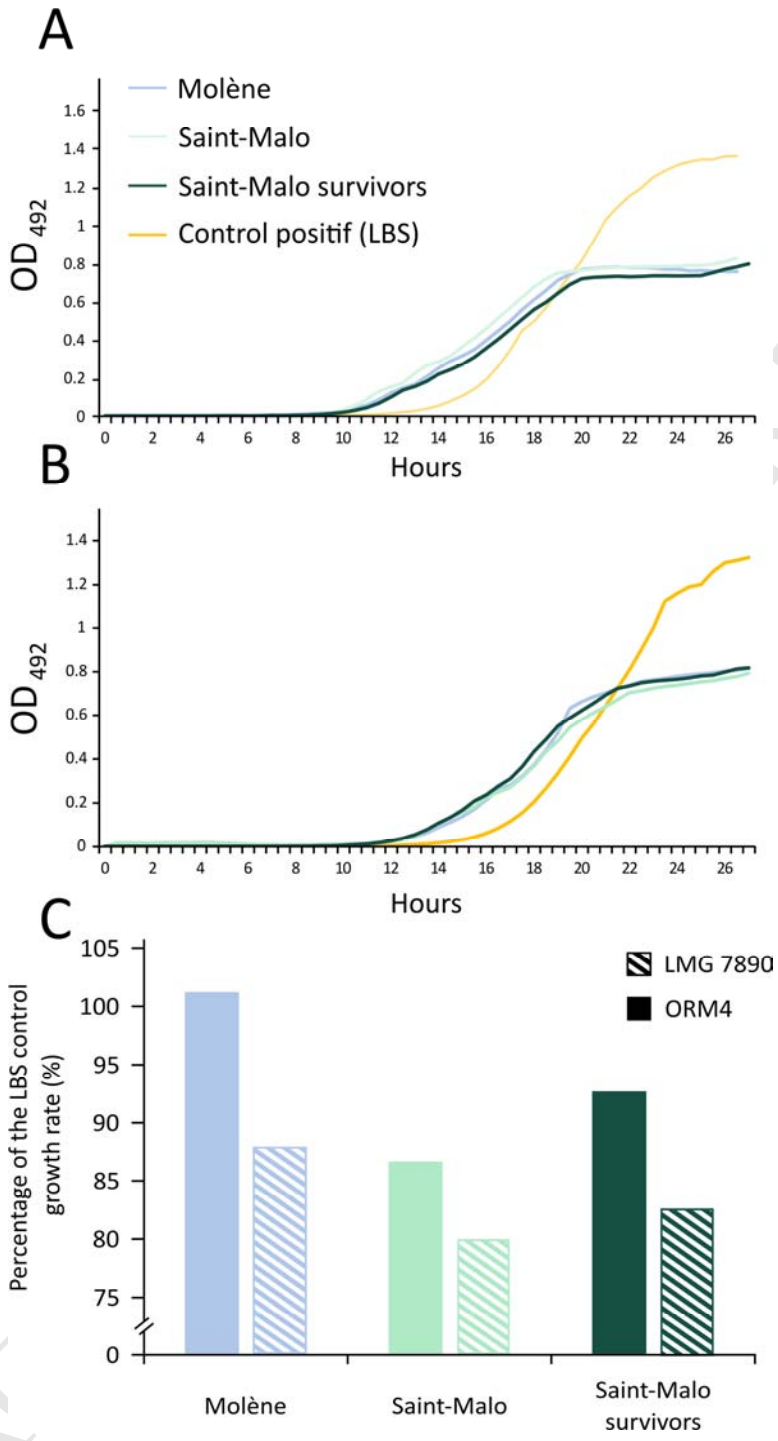

359

Fig. 7: Growth curves of the (A) non-virulent strain LMG7890 and (B) the virulent strain ORM4 in the serum of abalones. The growth of the bacteria in LBS was used as a positive control. (C) Growth rate of the LMH7890 and ORM4 strains in abalone serum are expressed as a percentage of the maximum growth rate in the LBS control.

360

361 **4. Discussion**

Populations exposed to contrasting environmental conditions and having different disease occurrences can evolve different susceptibilities against a particular pathogen. Based on this hypothesis, two populations of *H. tuberculata* were chosen to examine how response to infection to *V. harveyi* could vary in abalone of different origins. In Saint-Malo, where the average sea water temperatures exceed 17°C during the summer spawning period, conditions are favorable for disease development and indeed, this population has been frequently impacted by disease [10]. On the other hand, mortality has never been reported in Molène and the surrounding region, where temperatures of 17°C are rarely observed[9]. Successive infections conducted with abalones from each of these two natural populations showed marked differences in survival. Following 24 days after a first exposure to *V. harveyi*, a survival rate of 51% was observed for abalone from Molène and 95% for abalone from Saint-Malo (Fig. 1). Interestingly, the survival rate for Saint-Malo was not statistically different from that of uninfected controls. Our experimental infections confirm the hypothesis that abalone from a site that has experienced recurrent mortality (Saint-Malo) shows improved survival following infection with *V. harveyi*. According to Coustau and Théron (2004), resistance is defined as a relative term which indicates that a group exhibits a significantly better ability to prevent infection by a specific pathogen. Thus, all subsequent analyses were performed to identify mechanisms which could explain the resistance to the disease observed in abalone from Saint-Malo.

Differences in survival of *H. tuberculata* following successive infection with *V. harveyi* (10^6 bacteria/mL; 19°C) has been previously observed in farmed abalones [17]. Survival rate improved from 36% after a first infection to 56% following a second exposure, revealing different levels of resistance to the disease within the farmed population and a better ability to resist a second infection. While reduced mortality in this experiment may have been due to immune priming, the enhanced resistance observed at the second exposure could also be explained as an elimination of susceptible phenotypes following the first infection. In order to isolate a priming effect, improved response to the disease needs to be observed in conditions where potentially susceptible phenotypes are not eliminated at a first infection. Therefore, in the present experiment, mild infection conditions in term of both temperature (18°C) and bacterial concentration (10^4 bacteria/mL) were used to avoid mortality after a first exposure to *V. harveyi,* which was the case for the Saint-Malo population. Despite these infection conditions, survival was low in the susceptible population of Molène. Thus, these infection conditions allowed on one hand, to discriminate the two populations in term of resistance, and on the

other hand, to discern which parameters allowed improved resistance to the disease in abalone from Saint-Malo.

After the first infection with *V. harveyi*, individuals from both Saint-Malo and Molène suffered an important drop in phagocytosis (~40% compared to the control) after the first day of exposure, followed by a recovery of this activity by the third day, showing a similar response between the two populations in cellular immunity during the first infection (Fig. 3). The reduction in phagocytosis index could be explained by the saturation of a high proportion of haemocytes following active phagocytosis of *V. harveyi* in the early stages of exposure, resulting in less efficient bead engulfment by 24 hours post-infection. Alternatively, the observed reduction in phagocytosis could be interpreted as an inhibition of phagocytosis. Previous studies have shown that the ORM4 strain can perturb the MAPK signaling pathway by inhibiting phosphorylation of the p38 MAPK, leading to inhibition of phagocytosis compared to the non-pathogenic strain of *V. harveyi* (LM7890)[16]. Moreover, a significant decrease in phagocytosis index 24 hours after exposure to *V. harveyi* is linked with a downregulation of clathrin, a protein involved in endocytosis [15]. Therefore, the lower phagocytosis index observed is likely due to an inhibition of phagocytosis induced by the pathogen.

Interestingly, no significant decrease in phagocytosis was observed 1 day after the second exposure for abalones from Saint-Malo (Fig. 3A). The response of this population to the second infection can be interpreted as an immune priming effect. The survival rates observed in the control and infected conditions in Saint-Malo were similar, supporting the interpretation that the improved response to an infection can be due to a priming effect rather than an elimination of susceptible phenotypes. For the Molène population, low survival rates following the first infection preclude such interpretation.

Immune priming allows invertebrates to show improved survival to a pathogen following a first infection. This mechanism is now known in several insect species [30–32] and the freshwater snail *Biomphalaria glabrata* [20,33]. In the marine realm, immune priming was first examined in copepods [34]. More recently, examples among a few marine molluscs have also been documented: *Chlamys farreri* [35], *Mytilus galloprovincialis* [36] and *Crassostrea gigas* [37]. In the gastropod *Biomphalaria glabrata,* a species phylogenetically close to *H. tuberculata*, a first exposure to the trematode *Schistosoma mansoni* conferred an immune priming effect which led to complete protection, such that a secondary infection exhibited animals with a parasite prevalence of 0% for primed individuals compared to 100% for unprimed [20]. In the Pacific oyster *C. gigas*, a more acute and rapid immune response in term of phagocytosis and hematopoiesis was

observed after being primed with heat-killed *Vibrio splendidus* 7 days before the infection [35]. Since phagocytosis is usually the first response of the host against the pathogen, inhibition of this mechanism is a widespread strategy among pathogens to persist inside the host tissues [38]. Early phagocytosis response can then be crucial for the resistance of animals against infection and septicemia. In the case of *H. tuberculata*, the first exposure can act as an immune treatment that prevents future phagocytosis inhibition in abalone, thereby improving the early response to a subsequent exposure. A priming effect could allow the abalone immune system to be stimulated in the field at the beginning of the mortality season, thus enhancing protection for the rest of the critical period.

Because of the importance of the phagocytic response, and its implication in priming effect, this immune mechanism has been further examined. During the experimental infections, host phagocytosis was quantified using fluorescent beads. This commonly used approach [16] shows the activity of haemocytes rather than the actual ability to phagocytose a specific bacterium cell. While actual internalization of *V. harveyi* cells has previously been shown in primary cultured cells of farmed abalone haemolymph and gills [26], 3D fluorescent microscopy was used to confirm that this was the case in the freshly collected haemolymph from abalone from both Saint-Malo and Molène. Fluorescent microscopy shows that GFP-labelled bacterial cells are clearly observed inside the haemocytes, providing unquestionable evidence of internalization of *V. harveyi* by the haemocytes of *H. tuberculata* (Fig. 5) and confirming that subsequent flow cytometry measurements made with GFP-labelled *V. harveyi* quantifies actual phagocytosis. Phagocytosis of GFP-labelled bacteria performed two months after the infection experiment on uninfected individuals exhibited similar responses between the two populations. Abalones from Saint-Malo and Molène showed the same phagocytosis capacity and the same response to the ECPs. Indeed, the two populations suffer a phagocytosis inhibition of about 20% when exposed to 30 $\mu g.ml^{-1}$ of ECPs relative to the to the 0 $\mu g.ml^{-1}$ controls (Fig. 6). However, for the abalone from Saint-Malo surviving the successive infections, no statistical difference was observed between phagocytosis index exposed to concentrations of 0 µg, 15 $\mu g.ml^{-1}$ and 30 $\mu g.ml^{-1}$ of ECPs, suggesting a potential long-term priming effect against the inhibition of phagocytosis induced by ECPs. This result indicates that the protection against phagocytosis inhibition induced by the first exposure has persisted for over two months.

Our results are the first to indicate the existence of immune priming in abalones, however, the present study does not differentiate between the two possible types of priming. Immune priming in invertebrates occurs either as a sustained response of immune mechanisms which prevents a subsequent attack, or via a

specific response which allows recognition of the pathogen thus inducing a more intensive and rapid immune response [20]. Future work addressing whether sustained response or specificity of response is present in abalone could further our understanding of how immune priming acts in this species. For example, the injection of heat-killed bacteria could address whether immune priming is a specific response in *H. tuberculata*, as performed with the Pacific oyster [37]. Enhanced phagocytosis was observed only in oysters injected with heat-killed *V. splendidus*, but not with 4 other species of bacteria, suggesting specific recognition of this pathogen. The injection of heat-killed bacteria would also allow the induction of a more intensive immune effect by delivering higher doses of the pathogen. The infection performed in the present study was weak to avoid mortality, possibly leading to a partial or diminished immune priming response.

Sustained immune response is another possible mechanism of immune priming. The pathogenic strain of *V. harveyi* ORM4 is able to avoid the bactericidal response of abalone through an inhibition of the activity of the p38 MAPK, a MAP kinase which is thought to trigger a number of immune responses such as phagocytosis or the secretion of reactive oxygen species [16]. This kind of virulence has also been shown in other marine models. For example, the secretion of a metalloprotease by *Vibrio aestuarianus*, a pathogen of the Pacific oyster *C. gigas*, inhibits, among other immune parameters, phagocytosis [39]. Proteases secreted by the pathogen are a common mechanisms for the inhibition of phagocytosis, but can be counter-acted by protease inhibitors produced by the host [40]. In the disk abalone *Haliotis discus discus*, three types of clade B serine protease inhibitors are expressed in haemocytes following injection of *V. parahaemolyticus* or of LPS [41]. Sustained synthesis of protease inhibitors by *H. tuberculata* may therefore be a possible explanation of the long-term protection against phagocytosis inhibition. Future work quantifying protease inhibitors following successive infections with *V. harveyi* could confirm this hypothesis.

Humoral effectors may also contribute to the resistance of the Saint-Malo abalone to *V. harveyi* infection. Marine invertebrates possess a large set of antimicrobial peptides that can counteract bacterial growth [42]. Hemocyanin can also have strong antimicrobial activity [43], while other factors can limit bacterial growth by sequestering or limiting the availability of nutrients such as iron [44]. In the European abalone, the onset of growth of the two bacterial strains occurred 2-3 hours earlier in the serum of abalone than the LBS control, irrespective of the population, showing potential activators of bacterial growth may be present in the abalone serum. Moreover, bacterial growth rate was greater for the virulent strain of *V. harveyi* (ORM4) compared to the non-virulent strain LMG 7890 (Fig. 7). However, maximum growth rate of the virulent strain

ORM4 was lower in the haemolymph of Saint-Malo compared to Molène, indicating that the serum of abalone from Saint-Malo is less favorable for ORM4 growth. Therefore, resistance to *V. harveyi* in abalone from Saint-Malo may in part be explained by the ability to slow down bacterial growth within the serum. Host fluids can have significant effects in growth and gene expression of bacteria [45,46]. For example, the pedal mucus of the small abalone *Haliotis diversicolor* has been showed to induce the formation of a biofilm by *Vibrio alginolyticus* and to enhance the density of bacteria [46]. In the present work, bacterial growth in the serum was measured two months after the successive infections; it is possible that different responses may be observed during infection with *V. harveyi*.

The most striking differences between the resistant and susceptible populations were observed in the detection of *V. harveyi* in the haemolymph and the gills of abalone. In the haemolymph, *V. harveyi* was detected in only 5 individuals, all from the Molène population (Fig. 4A). Despite the low survival rate in abalone from Molène, the small number of individuals positive for *V. harveyi* can be explained by the rapid growth rate of *V. harveyi* in abalone serum (~10 hours, see Fig 7), rendering the time frame to detect the bacteria in hemolymph (between the beginning of exponential phase and septicemia) very short. It is nevertheless interesting to note that all individuals for which *V. harveyi* was detected were from Molène, suggesting that *V. harveyi* is better able to penetrate the haemolymph of abalone from this population. The results of THC support this interpretation. Although no differences in THC were observed between infected abalones and uninfected controls in the Saint-Malo population, abalone from Molène showed a significant increase of the number of circulating haemocytes after 24 hours of exposure to *V. harveyi* (Fig. 2). This likely denotes an inflammatory response by a recruitment of haemocytes in the hemocoel suggesting greater presence of *V. harveyi* in this compartment in abalone from Molène.

Detection of *V. harveyi* in the gills was significantly greater in abalone from Molène compared to Saint-Malo (Fig. 4B), and a binomial regression showed that the detection of *V. harveyi* on the gills was correlated with an increase of THC and a decrease of phagocytosis index (Table. 1). These findings indicate that even if the bacterium is not detected in the haemolymph, its presence in the gills already induces an immune response. The portal of entry of *V. harveyi* is the gills of abalones [47], where previous work has shown that bacterial density can be 5-fold greater in the gills compared to other tissues 6 hours after exposure. The small number of individuals which were positive for *V. harveyi* in the gills among abalone from Saint-Malo suggests that an important part of the resistance of this population may depend on the ability to prevent the settlement and

penetration of bacteria in the gills. The ability to adhere to the portal of entry of the host can be essential for the virulence of a bacterium. This is the case of *Flavobacterium colunmare* and *Yersinia ruckeri*, for which all known virulent strains are able to adhere to the gills of their respective hosts, whereas non-virulent strains cannot [48,49]. Preventing settlement of bacteria on the gills may be an important defense mechanism against disease. Other strategies can also be used to counteract the settlement of bacteria on the gills of marine invertebrates, such as the localized production of lysozyme or antimicrobial peptides. In the penaid shrimp *Marsupenaeus japonicas,* lysozyme expression and antimicrobial activity are elevated in the gills [50]. Moreover, an antimicrobial peptide expressed only in gills has been discovered in the abalone *Haliotis discus* [51]. Since the gills may be important in the resistance to *V. harveyi* infection, future work comparing potential antimicrobial or anti-adherent activity in the gills of abalone from the two populations may help to identify the mechanisms by which abalone from Saint-Malo have enhanced resistance against *V. harveyi*.

Surprisingly, no individuals were positive for *V. harveyi* in the gills 3 days after the first exposure in both populations. This is possibly due to the fact that bacterial concentrations fluctuate over the course of the experimental infection, as was quantified in similar experiments [22]. Thus, bacterial concentrations at this given time point may have fallen below the detection limit.

5. Conclusions

This study shows the differential resistance between the two populations of *H. tuberculata* against *V. harveyi* and the comparisons between these two populations identified a number of resistance effectors. Abalone haemolymph exhibited weak defenses against the bacteria, and are presumably insufficient to contain a septicemia, although phagocytosis and limitation of bacterium growth in the serum are two possible resistance mechanisms. On the other hand, the significant differences observed in detection of *V. harveyi* in the gills point towards an important implication of the gills in the resistance of the Saint-Malo population. Our results show the first evidence of immune priming in *Haliotis tuberculata* and the enhanced capacity of phagocytosis at the second infection demonstrate a potential importance of cellular response against *V. harveyi*. A synergistic interaction among effectors in the gills and haemolymph likely lead to disease resistance. Further work is needed to understand precisely how the population of Saint-Malo resists infection and to find the gills effectors that counteract the settlement of *V. harveyi* in abalone gills.

Acknowledgments

This work was supported by the "Laboratoire d'Excellence" LabexMER (ANR-10-LABX-19) and co-funded by a grant from the French government under the program "Investissements d'Avenir". The authors are grateful to RIERA Fabien; RICHARD Gaelle; HARNEY Ewan; LAISNEY Naïda; PETINAY Stephanie for their help in sampling during the infections experiment, and BIDAULT Adeline her assistance and suggestions for qPCR analyses. Finally, authors are also grateful to all the SMEL team for their help and their warm welcome within their structure.

References

[1] S. Altizer, D. Harvell, E. Friedle, Rapid evolutionary dynamics and disease threats to biodiversity, Trends Ecol. Evol. 18 (2003) 589–596. doi:10.1016/j.tree.2003.08.013.

[2] L. Wilfert, F.M. Jiggins, The dynamics of reciprocal selective sweeps of host resistance and a parasite counter-adaptation in drosophila, Biol. Lett. 6 (2010) 666–8. doi:10.1098/rsbl.2010.0329.

[3] C.D. Harvell, C. E.Mitchell, R.W. Jessica, A. Sonia, P.D. Andrew, R. S.Ostfeld, et al., Climate warming and disease risks for terrestrial and marine biota, Science (80-.). 296 (2002) 2158–2162. doi:10.1126/science.1063699.

[4] W. Cheng, I.S. Hsiao, C.-H. Hsu, J.C. Chen, Change in water temperature on the immune response of Taiwan abalone *Haliotis diversicolor* supertexta and its susceptibility to *Vibrio parahaemolyticus*, Dis. Aquat. Organ. 60 (2004) 157–164. doi:10.1016/j.fsi.2004.03.007.

[5] L. Vezzulli, I. Brettar, E. Pezzati, P.C. Reid, R.R. Colwell, M.G. Höfle, et al., Long-term effects of ocean warming on the prokaryotic community: evidence from the vibrios, ISME J. 6 (2012) 21–30. doi:10.1038/ismej.2011.89.

[6] K.K. Lee, P.C. Liu, Y.C. Chen, C.Y. Huang, The implication of ambient temperature with the outbreak of vibriosis in cultured small abalone *Haliotis diversicolor* supertexta Lischke, J. Therm. Biol. 26 (2001) 585–587. doi:10.1016/S0306-4565(01)00004-3.

[7] M. Monari, V. Matozzo, J. Foschi, O. Cattani, G.P. Serrazanetti, M.G. Marin, Effects of high temperatures on functional responses of haemocytes in the clam *Chamelea gallina*, Fish Shellfish Immunol. 22 (2007) 98–114. doi:10.1016/j.fsi.2006.03.016.

[8] J.L. Nicolas, O. Basuyaux, J. Mazurié, A. Thébault, *Vibrio* carchariae, a pathogen of the abalone *Haliotis*

564 *tuberculata*, Dis. Aquat. Organ. 50 (2002) 35–43. doi:10.3354/dao050035.

565 [9] A. Thébault, Bilan 1998 du Réseau REPAMO, 1998.

566 [10] S. Huchette, J. Clavier, status of the ormer (*haliotis tuberculata L.*) industry in europe, J. Shellfish Res. 23

567 (2004) 951 – 955.

568 [11] M.-A. Travers, O. Basuyaux, N. Le Goïc, S. Huchette, J.-L. Nicolas, M. Koken, et al., Influence of

569 temperature and spawning effort on *Haliotis tuberculata* mortalities caused by *Vibrio harveyi* : an

570 example of emerging vibriosis linked to global warming, Glob. Chang. Biol. 15 (2009) 1365–1376.

571 doi:10.1111/j.1365-2486.2008.01764.x.

572 [12] M.-A. Travers, N. Le Goïc, S. Huchette, M. Koken, C. Paillard, Summer immune depression associated

573 with increased susceptibility of the European abalone, *Haliotis tuberculata* to *Vibrio harveyi infection*,

574 Fish Shellfish Immunol. 25 (2008) 800–808. doi:10.1016/j.fsi.2008.08.003.

575 [13] M. Cardinaud, C. Offret, S. Huchette, D. Moraga, C. Paillard, The impacts of handling and air exposure

576 on immune parameters, gene expression, and susceptibility to vibriosis of European abalone *Haliotis*

577 *tuberculata*, Fish Shellfish Immunol. 36 (2014) 1–8. doi:10.1016/j.fsi.2013.09.034.

578 [14] M. Collins, R. Knutti, J. Arblaster, J.-L. Dufresne, T. Fichefet, P. Friedlingstein, et al., Long-term Climate

579 Change: Projections, Commitments and Irreversibility, Clim. Chang. 2013 Phys. Sci. Basis. Contrib. Work.

580 Gr. I to Fifth Assess. Rep. Intergov. Panel Clim. Chang. (2013) 1029–1136.

581 doi:10.1017/CBO9781107415324.024.

582 [15] M. Cardinaud, N.M. Dheilly, S. Huchette, D. Moraga, C. Paillard, The early stages of the immune

583 response of the European abalone *Haliotis tuberculata* to a *Vibrio harveyi* infection, Dev. Comp.

584 Immunol. 51 (2015) 287–297. doi:10.1016/j.dci.2015.02.019.

585 [16] M.-A. Travers, R. Le Bouffant, C.S. Friedman, F. Buzin, B. Cougard, S. Huchette, et al., Pathogenic vibrio

586 harveyi, in contrast to non-pathogenic strains, intervenes with the p38 MAPK pathway to avoid an

587 abalone haemocyte immune response, J. Cell. Biochem. 106 (2009) 152–160. doi:10.1002/jcb.21990.

588 [17] M.-A. Travers, A. Meistertzheim, M. Cardinaud, C.S. Friedman, S. Huchette, D. Moraga, et al., Gene

589 expression patterns of abalone, Haliotis tuberculata, during successive infections by the pathogen

590 Vibrio harveyi, J. Invertebr. Pathol. 105 (2010) 289–297. doi:10.1016/j.jip.2010.08.001.

591 [18] C.S. Friedman, N. Wight, L.M. Crosson, G.R. VanBlaricom, K.D. Lafferty, Reduced disease in black

592 abalone following mass mortality: Phage therapy and natural selection, Front. Microbiol. 5 (2014) 1–10.

doi:10.3389/fmicb.2014.00078.

[19] J. Kurtz, Specific memory within innate immune systems, Trends Immunol. 26 (2005) 186–192. doi:10.1016/j.it.2005.02.001.

[20] J. Portela, D. Duval, A. Rognon, R. Galinier, J. Boissier, C. Coustau, et al., Evidence for specific genotype-dependent immune priming in the lophotrochozoan Biomphalaria glabrata snail., J. Innate Immun. 5 (2013) 261–76. doi:10.1159/000345909.

[21] Y. Moret, Trans-generational immune priming": specific enhancement of the antimicrobial immune response in the mealworm beetle, Tenebrio molitor., Proc. Biol. Sci. 273 (2006) 1399–405. doi:10.1098/rspb.2006.3465.

[22] M.-A. Travers, A. Barbou, N. Le Goïc, S. Huchette, C. Paillard, M. Koken, Construction of a stable GFP-tagged *Vibrio harveyi* strain for bacterial dynamics analysis of abalone infection., FEMS Microbiol. Lett. 289 (2008) 34–40. doi:10.1111/j.1574-6968.2008.01367.x.

[23] D. Schikorski, T. Renault, C. Paillard, D. Tourbiez, D. Saulnier, Development of TaqMan real-time PCR assays for monitoring *Vibrio harveyi* infection and a plasmid harbored by virulent strains in European abalone *Haliotis tuberculata* aquaculture, 395 (2013) 106–112. doi:10.1016/j.aquaculture.2013.02.005.

[24] P. V Liu, Survey of hemolysin production among species of pseudomonas, Infect. Immun. (1957) 718–727.

[25] L.S. Ramagli, 2-D Proteome Analysis Protocols, in: A.J. Link (Ed.), Humana Press, Totowa, NJ, 1999: pp. 99–103. doi:10.1385/1-59259-584-7:99.

[26] D. Pichon, B. Cudennec, S. Huchette, Characterization of abalone Haliotis tuberculata–Vibrio harveyi interactions in gill primary cultures, Cytotechnology. (2013) 759–772. doi:10.1007/s10616-013-9583-1.

[27] T.M. Therneau, A Package for Survival Analysis in S, (2015). http://cran.r-project.org/package=survival.

[28] R Core Team, R: A Language and Environment for Statistical Computing, (2015). https://www.r-project.org/.

[29] C. Coustau, A. Théron, Resistant or resisting: seeking consensus terminology, Trends Parasitol. 20 (2004) 208–209. doi:10.1016/j.pt.2004.02.006.

[30] G. Wu, M. Li, Y. Liu, Y. Ding, Y. Yi, The specificity of immune priming in silkworm, *Bombyx mori*, is mediated by the phagocytic ability of granular cells, J. Insect Physiol. 81 (2015) 60–68. doi:10.1016/j.jinsphys.2015.07.004.

622 [31] G. Wu, Z. Zhao, C. Liu, L. Qiu, Priming *Galleria mellonella* (Lepidoptera: Pyralidae) Larvae With Heat-
623 Killed Bacterial Cells Induced an Enhanced Immune Protection Against *Photorhabdus luminescens* TT01
624 and the Role of Innate Immunity in the Process, (2004) 2–5.
625 [32] Z. Zhao, G. Wu, J. Wang, C. Liu, L. Qiu, Next-generation sequencing-based transcriptome analysis of
626 *Helicoverpa armigera* larvae immune-primed with *Photorhabdus luminescens* TT01, PLoS One. 8 (2013)
627 e80146. doi:10.1371/journal.pone.0080146.
628 [33] S. Pinaud, J. Portela, D. Duval, F.C. Nowacki, M.A. Olive, J.F. Allienne, et al., A Shift from Cellular to
629 Humoral Responses Contributes to Innate Immune Memory in the Vector Snail *Biomphalaria glabrata*,
630 PLoS Pathog. 12 (2016) 1–18. doi:10.1371/journal.ppat.1005361.
631 [34] J. Kurtz, K. Franz, Evidence for memory in invertebrate immunity., Nature. 425 (2003) 37–38.
632 doi:10.1038/425037a.
633 [35] M. Cong, L. Song, L. Wang, J. Zhao, L. Qiu, L. Li, et al., The enhanced immune protection of Zhikong
634 scallop *Chlamys farreri* on the secondary encounter with *Listonella anguillarum*, Comp. Biochem.
635 Physiol. - B Biochem. Mol. Biol. 151 (2008) 191–196. doi:10.1016/j.cbpb.2008.06.014.
636 [36] C. Ciacci, B. Citterio, M. Betti, B. Canonico, P. Roch, L. Canesi, Functional differential immune responses
637 of *Mytilus galloprovincialis* to bacterial challenge, Comp. Biochem. Physiol. - B Biochem. Mol. Biol. 153
638 (2009) 365–371. doi:10.1016/j.cbpb.2009.04.007.
639 [37] T. Zhang, L. Qiu, Z. Sun, L. Wang, Z. Zhou, R. Liu, et al., The specifically enhanced cellular immune
640 responses in Pacific oyster (*Crassostrea gigas*) against secondary challenge with *Vibrio splendidus*, Dev.
641 Comp. Immunol. 45 (2014) 141–150. doi:10.1016/j.dci.2014.02.015.
642 [38] B. Allam, D. Raftos, Immune responses to infectious diseases in bivalves, J. Invertebr. Pathol. 131 (2015)
643 121–136. doi:10.1016/j.jip.2015.05.005.
644 [39] Y. Labreuche, F. Le Roux, J. Henry, C. Zatylny, A. Huvet, C. Lambert, et al., *Vibrio aestuarianus zinc*
645 metalloprotease causes lethality in the Pacific oyster *Crassostrea gigas* and impairs the host cellular
646 immune defenses, Fish Shellfish Immunol. 29 (2010) 753–758. doi:10.1016/j.fsi.2010.07.007.
647 [40] P.B. Armstrong, Proteases and protease inhibitors: a balance of activities in host-pathogen interaction,
648 Immunobiology. 211 (2006) 263–281. doi:10.1016/j.imbio.2006.01.002.
649 [41] S.D.N.K. Bathige, N. Umasuthan, G.I. Godahewa, I. Whang, C. Kim, H.C. Park, et al., Three novel clade B
650 serine protease inhibitors from disk abalone, *Haliotis discus discus*: Molecular perspectives and

responses to immune challenges and tissue injury, Fish Shellfish Immunol. 45 (2015) 334–341. doi:10.1016/j.fsi.2015.04.020.

[42] J. Tincu, S. Taylor, Antimicrobial peptides from marine invertebrates, Antimicrob. Agents Chemother. 48 (2004) 3645–3654. doi:10.1128/AAC.48.10.3645.

[43] P. Dolashka, Moshtanska, A. Dolashki, J. Van Beeumen, M. Floetenmeyerd, L. Velkova, et al., Antimicrobial Activity of Molluscan Hemocyanins from *Helix* and *Rapana* Snails, Curr. Pharm. Biotechnol. 16 (2015) 1–1. doi:10.2174/1389201016666150907113435.

[44] C.P. Doherty, Host-pathogen interactions: the role of iron., J. Nutr. 137 (2007) 1341–1344.

[45] A.M. Staroscik, D.R. Nelson, The influence of salmon surface mucus on the growth of Flavobacterium columnare, J. Fish Dis. 31 (2008) 59–69. doi:10.1111/j.1365-2761.2007.00867.x.

[46] F. Guo, Z. bin Huang, M. qin Huang, J. Zhao, C. huan Ke, Effects of small abalone, *Haliotis diversicolor*, pedal mucus on bacterial growth, attachment, biofilm formation and community structure, Aquaculture. 293 (2009) 35–41. doi:10.1016/j.aquaculture.2009.03.033.

[47] M. Cardinaud, A. Barbou, C. Capitaine, A. Bidault, A.M. Dujon, D. Moraga, et al., Vibrio harveyi adheres to and penetrates tissues of the European abalone Haliotis tuberculata within the first hours of contact, Appl. Environ. Microbiol. 80 (2014) 6328–6333. doi:10.1128/AEM.01036-14.

[48] E. Tobback, A. Decostere, K. Hermans, W. Van den Broeck, F. Haesebrouck, K. Chiers, In vitro markers for virulence in *Yersinia ruckeri*, J. Fish Dis. 33 (2010) 197–209. doi:10.1111/j.1365-2761.2009.01106.x.

[49] O. Olivares-Fuster, S.A. Bullard, A. McElwain, M.J. Llosa, C.R. Arias, Adhesion dynamics of *Flavobacterium columnare* to channel catfish *Ictalurus punctatus* and zebrafish *Danio rerio* after immersion challenge, Dis. Aquat. Organ. 96 (2011) 221–227. doi:10.3354/dao02371.

[50] A. Kaizu, F.F. Fagutao, H. Kondo, T. Aoki, I. Hirono, Functional analysis of C-type lysozyme in penaeid shrimp, J. Biol. Chem. 286 (2011) 44344–44349. doi:10.1074/jbc.M111.292672.

[51] J.-K. Seo, H.-J. Go, C.-H. Kim, B.-H. Nam, N.G. Park, Antimicrobial peptide, hdMolluscidin, purified from the gill of the abalone, *Haliotis discus*, Fish Shellfish Immunol. 52 (2016) 289–297. doi:10.1016/j.fsi.2016.03.150.

679 **Captions**

680 **Figure 1:** Kaplan-Meier survival rate following the first exposure of the two populations to 10^4
681 bacteria/mL during 24 hours at 18°C

682 **Figure 2:** Total haemocytes count (THC) during the two exposures of (A) Saint-Malo and (B) Molène.
683 Red dots indicate the exposures. ND indicates that no data is available.* indicates values that are
684 significantly different from the control for a pairwise comparison of the least-squares means ($p <$
685 0.05).

686 **Figure 3:** Phagocytosis index based on micro-beads engulfment (percentage of haemocytes
687 containing three or more fluorescent beads relative to total haemocytes) during two successive
688 infections of abalone from (A) Saint-Malo and (B) Molène. Red dots indicate the timing of bacterial
689 exposure. ND indicates that no data is available.* indicates values that are significantly different from
690 the control for a pairwise comparison of the least-squares means ($p < 0.05$).
691 **Figure 4:** Percentage of positive individuals for *V.harveyi* (n=9) in (A) haemolymph and (B) gills
692 obtained by qPCR using specific primers and a TaqMan probe. The number 0 indicates that no
693 individuals were found as positive at a given population and time point. Red dots indicate the timing
694 of bacterial exposure. ND indicates that no data is available.
695 **Figure 5:** 3-dimensional fluorescence microscopy (x60) pictures of a haemocyte (cytoskeleton in
696 orange and nucleus in blue) which has phagocyted GFP-labelled V. harveyi (green). The central
697 picture (B) shows a reconstruction of 14 stacked fluorescence images. The flanking pictures show
698 cross-sections compiled along the (A) z-axis and (C) x-axis.

699 **Figure 6:** Impact of two concentrations of extracellular products of *V. harveyi* (15µg/mL and 30
700 µg/mL) on phagocytosis of GFP-labelled bacteria. Values are the means of green fluorescence
701 emitted by haemocytes. * indicates values that are significantly different from condition without
702 ECPs for a pairwise comparison of the least-squares means (*$P < 0.05$, **$P < 0.01$, ***$P < 0.001$).
703 **Figure 7:** Growth curves of the (A) non-virulent strain LMG7890 and (B) the virulent strain ORM4 in

the serum of abalones. The growth of the bacteria in LBS was used as a positive control. (C) Growth rate of the LMH7890 and ORM4 strains in abalone serum are expressed as a percentage of the maximum growth rate in the LBS control.